Robotica (2012) volume 30, pp. 39–51. © Cambridge University Press 2011
doi:10.1017/S0263574711000397

Modeling and gait selection of passivity-based seven-link bipeds with dynamic series of walking phases

Yan Huang†, Qining Wang†,*, Baojun Chen†, Guangming Xie† and Long Wang†

†*Intelligent Control Laboratory, College of Engineering, Peking University, Beijing 100871, China*

(Received in Final Form: March 22, 2011. First published online: April 26, 2011)

SUMMARY

This paper presents a seven-link dynamic walking model that is more close to human beings than other passivity-based dynamic walking models. We add hip actuation, upper body, flat feet, and ankle joints with torsional springs to the model. Walking sequence of flat-feet walkers has several substreams, which forms bipedal walking with dynamic series of phases. We investigate the effects of ankle stiffness on gait selection and evaluate different gaits in walking velocity, efficiency, and stability. Experimental results indicate that ankle stiffness plays different roles in different gaits and the gaits, which are more close to human walking with moderate speed, achieve better motion characteristics.

KEYWORDS: Passive dynamic walking; Bipeds; Gait selection; Ankle stiffness; Dynamic walking phases.

1. Introduction

Human beings can achieve stable and efficient dynamic bipedal walking on various different terrains without much effort. Though people's usual gaits tend to be natural and simple, bipedal walking involves highly nonlinear and multivariable dynamics with discrete events and a varying configuration. To study human locomotion and construct bipedal robots, the trajectory-control approach has been proposed.[1] By controlling joint angles precisely, the humanoid robots can achieve static equilibrium postures at any time during motion. In such static walking gaits, the zero moment point (ZMP) has to be within the convex hull of the supporting area.[2] However, the corresponding energy consumption and requirements of actuators are relatively high.

Different from static walking, dynamic bipedal walkers may not reach static equilibrium at some time, but can realize stable cyclic walking. As an example, passive dynamic walking[3] has been presented as a possible explanation for the efficiency of the human gait, which showed that a mechanism with two legs can be constructed so as to descend a gentle slope with no actuation and no active control. Several studies reported that these kinds of walking machines work with reasonable stability over a range of slopes[3–5] and on level ground with kinds of actuation added.[6–9] Dynamic walking achieves high efficiency and shows a remarkable resemblance to the human gait.

Most studies of passive dynamic walking are based on the Simplest Walking Model proposed by Garcia *et al*.[10] and extended work by Kuo,[11] which consist of two rigid massless legs connected by a frictionless hinge at the hip, with a large point mass at the hip and a small mass at each foot (placed at the ankle). In these models, passive walkers are often modeled with point feet or round feet, which have clear disadvantages of being unable to achieve the start and stop of walking. However, only a few studies have been done on a flat foot shape in passive dynamic models.[13–15] These studies proposed that the flat foot with a geometric parameter (foot length) can introduce a toe-strike collision in addition to the heel-strike impulse and influence the passive dynamics of walking. In addition, compliant ankles have been added to passive dynamic walkers.[18,19] The mechanical energy stored in such elastic elements can be recovered as both kinetic and gravitational energies. It may improve the efficiency and adaptability of bipedal walking. Our recent study reported that dynamic walking models with flat feet and passive ankle springs can largely resemble real human walking.[16] However, in all these dynamic bipedal models, the walking phases are certain. It is different from real human walking.

In this paper, we present a seven-link dynamic walking model that is more close to human beings comparing with other passivity-based dynamic walking models. We add hip actuation, upper body, flat feet, and ankle joints with torsional springs to the model. Since flat-foot walker has multiple contact cases, the walking sequence is not predetermined, which is different from that of point-feet and round-feet walkers. Walking sequence of flat-feet walkers has several substreams, which forms bipedal walking with dynamic series of phases. Consequently, study on selection and comparison of different gaits will help us better understand motion characteristics of real human walking. Thus, we investigate the effects of ankle stiffness on gait selection and evaluated different gaits in walking velocity, efficiency, and stability.

This paper is organized as follows. Section 2 presents the dynamic walking model with flat feet and joint compliance in detail. Section 3 is devoted to describe the walking phases and different gaits. Section 4 gives the simulation results.

* Corresponding author. E-mail: qiningwang@pku.edu.cn

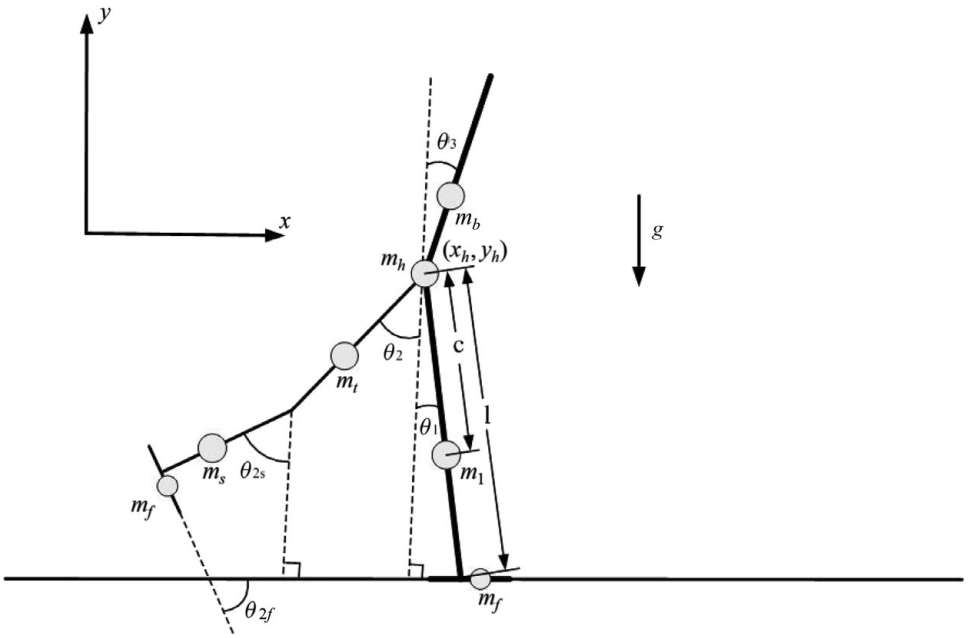

Fig. 1. Passivity-based dynamic bipedal walking model with flat feet and compliant ankle joints. The biped is powered by hip torque and ankle actuation. The thigh and the shank are connected at the knee joint, while the foot is mounted on the ankle with a torsional spring. Similar to Wisse *et al.*,[12] a kinematic coupling has been used in the model to keep the body midway between the two legs. The knee joints and ankle joints are modeled as passive joints that are constrained by torsional springs.

In Section 5, we discuss the effects of ankle stiffness on gait selection and compliant leg behavior. We conclude in Section 6.

2. Model

2.1. Bipedal model

To obtain further understanding of real human walking, we propose a passivity-based bipedal walking model that is more close to human beings than other passivity-based dynamic walking models. We add flat feet and compliant ankle joints to the model. As shown in Fig. 1, the two-dimensional model consists of two rigid legs interconnected individually through a hinge with a rigid upper body (mass added stick) connected at the hip. Each leg includes thigh, shank, and foot. The thigh and the shank are connected at the knee joint, while the foot is mounted on the ankle with a torsional spring. A point mass at hip represents the pelvis. The mass of each leg and foot is simplified as point mass added on the Center of Mass (CoM) of the shank, the thigh, and the foot, respectively.

Similar to Wisse *et al.*,[12] a kinematic coupling has been used in the model to keep the body midway between the two legs. In addition, our model adds compliance to the knee joints and ankle joints. Specifically, knee joints and ankle joints are modeled as passive joints that are constrained by torsional springs. The springs are mounted at the joints in the torsional way, which means that the torque generated by the spring is proportional to the deviation of the angle between links from the equilibrium position (see Fig. 2). To simplify the motion, we have several assumptions, including (1) shanks and thighs suffering no flexible deformation; (2) hip joint and knee joints with no damping or friction; (3) the friction between the walker and the ground is enough. Thus, the flat feet do not deform or slip; (4) strike is modeled as an instantaneous, fully inelastic impact where no slip and no bounce occurs. The bipedal walker travels forward on level ground with hip torque and ankle actuation.

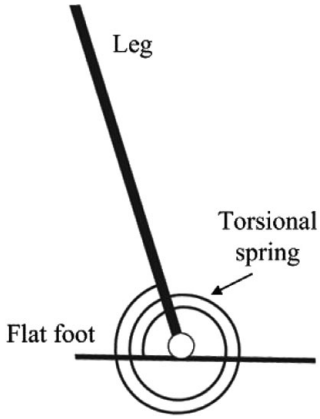

Fig. 2. Ankle joint with torsional spring. The torque generated by the spring is proportional to the deviation of the angle between links from the equilibrium position.

The stance leg keeps contact with ground while the swing leg pivots about the constraint hip. When the flat foot strikes the ground, there are two impulses, "heel-strike" and "foot-strike," representative of the initial impact of the heel and the following impact as the whole foot contacts the ground.[16,17] The shank of the stance foot is always locked and the whole leg can be modeled as one rigid stick, while the knee joint of the swing leg will release the shank immediately after foot-strike. The shank will be locked when it swings forward to a relatively small angle to the thigh.

https://doi.org/10.1017/S0263574711000397 Published online by Cambridge University Press

The bipedal walking is restricted to stop in three cases, including falling down, running, and shank releasing. We define that the walker falls down if the angle of either leg exceeds the normal range, which is from -1 rad to 1 rad in this study. And the model is considered to be running when the stance leg lifts up, which means that the ground force acted on the stance leg orthogonal to the floor decreases to zero, while the swing foot has no contact with ground. Shank releasing is the case that the shank of the swing leg is not locked before heel-strike. Foot scuffing, which means that the foot of the swing leg travels below the floor, often appears when the knee joint locks the shank too early. It is another case that the walker maybe have to stop. However, this case is likely avoided for a real three-dimensional walker with lateral motion. Thus, similar to other related studies,[12, 15, 16] we allow it if the foot travels below the floor not very seriously.

We suppose that the x-axis is along the ground while the y-axis is vertical to the ground upward. The configuration of the walker is defined by the coordinates of the point mass on hip joint and several angles, which include the swing angles between vertical axis and each thigh and shank, the angle between vertical axis and the upper body, and the foot angles between horizontal axis and each foot (see Fig. 1 for details), which can be arranged in a generalized vector $q = (x_h, y_h, \theta_1, \theta_2, \theta_3, \theta_{2s}, \theta_{1f}, \theta_{2f})^{\mathrm{T}}$. The positive directions of all the angles are counterclockwise. Note that the dimension of the generalized vector in different phases may be different. When the knee joint of the swing leg is locked, the freedom of the shank is reduced and the angle θ_{2s} is not included in the generalized coordinates. Consequently, the dimensions of mass matrix and generalized active force are also reduced in some phases.

2.2. *Dynamics of walking*

In the following paragraphs, we will focus on the Equation of Motion (EoM) of the proposed bipedal walking model. The model can be defined by the Euclidean coordinates x, which can be described by the x- and y-coordinates of the mass points and the corresponding angles (suppose leg 1 is the stance leg):

$$x = [x_h, y_h, x_{c1}, y_{c1}, \theta_1, x_{c2t}, y_{c2t}, \theta_2, x_{c3}, y_{c3}, \theta_3, x_{c2s}, y_{c2s}, \theta_{2s}, x_{c1f}, y_{c1f}, \theta_{1f}, x_{c2f}, y_{c2f}, \theta_{2f}]^{\mathrm{T}}. \quad (1)$$

The walker can also be described by the generalized coordinates q as mentioned before:

$$q = (x_h, y_h, \theta_1, \theta_2, \theta_3, \theta_{2s}, \theta_{1f}, \theta_{2f})^{\mathrm{T}}. \quad (2)$$

Defined matrix T as follows:

$$T = \mathrm{d}x/\mathrm{d}q \quad (3)$$

Thus, T transfers the velocities of the Euclidean coordinates $\dot{q}$ into the independent generalized coordinates $\dot{x}$. The mass matrix in rectangular coordinate x is defined as:

$$M = diag(m_h, m_h, m_l, m_l, I_l, m_t, m_t, I_t, m_b, m_b, I_b, m_s, m_s, I_s, m_f, m_f, I_f, m_f, m_f, I_f), \quad (4)$$

where m_h, m_l, m_t, m_b, m_s, and m_f are the masses of hip, each leg, each thigh, upper body, each shank, and each foot, respectively. I components are moments of inertia of corresponding parts. Since the mass of the model is distributed as point masses, the angles in x and the moments of inertia in M could be taken off for simplification.

Denote F as the active external force vector in rectangular coordinates. The constraint function is marked as $\xi(q)$, which is used to maintain foot contact with ground and detect impacts. Note that $\xi(q)$ in different walking phases may be different since the contact conditions change. For example, the constraint function $\xi(q)$ in the single-support phase (the full foot of the stance leg keeps contact with ground, as shown in Fig. 1) can be written as following:

$$\xi(q) = \begin{bmatrix} \theta_3 - \frac{1}{2}(\theta_1 + \theta_2) \\ x_h + l\sin\theta_1 - x_{\text{ankle}} \\ y_h - l\cos\theta_1 - l_{fh}\sin\theta_{1f} \\ y_h - l\cos\theta_1 + l_{ft}\sin\theta_{1f} \end{bmatrix}, \quad (5)$$

where x_{ankle} is the x-coordinate of the ankle of leg 1, l is leg length as shown in Fig. 1, and l_{fh} and l_{ft} are the distances from heel to ankle and from ankle to toe, respectively. Each component of $\xi(q)$ should keep zero to satisfy the contact condition. The contact of stance foot is modeled by one ground reaction force (GRF) along the floor and two GRFs perpendicular to the ground act on the two endpoints of the foot, respectively. If one of the forces perpendicular to the ground decreases below zero, the corresponding endpoint of the stance foot will lose contact with ground and the stance foot will rotate around the other endpoint. Each element of the constraint function corresponds to the generalized constrain force F_f.

We can obtain the EoM by Lagrange's equation of the first kind:

$$M_q\ddot{q} = F_q + \Phi^{\mathrm{T}}F_f, \quad (6)$$

$$\xi(q) = 0, \quad (7)$$

where $\Phi = \frac{\partial \xi}{\partial q}$. M_q is the mass matrix in the generalized coordinates:

$$M_q = T^{\mathrm{T}}MT. \quad (8)$$

F_q is the active external force in the generalized coordinates:

$$F_q = T^{\mathrm{T}}F - T^{\mathrm{T}}M\frac{\partial T}{\partial q}\dot{q}\dot{q}, \quad (9)$$

where F is the external force in the Euclidean coordinates. Equation (7) can be transformed to the followed equation:

$$\Phi\ddot{q} = -\frac{\partial(\Phi\dot{q})}{\partial q}\dot{q}. \quad (10)$$

https://doi.org/10.1017/S0263574711000397 Published online by Cambridge University Press

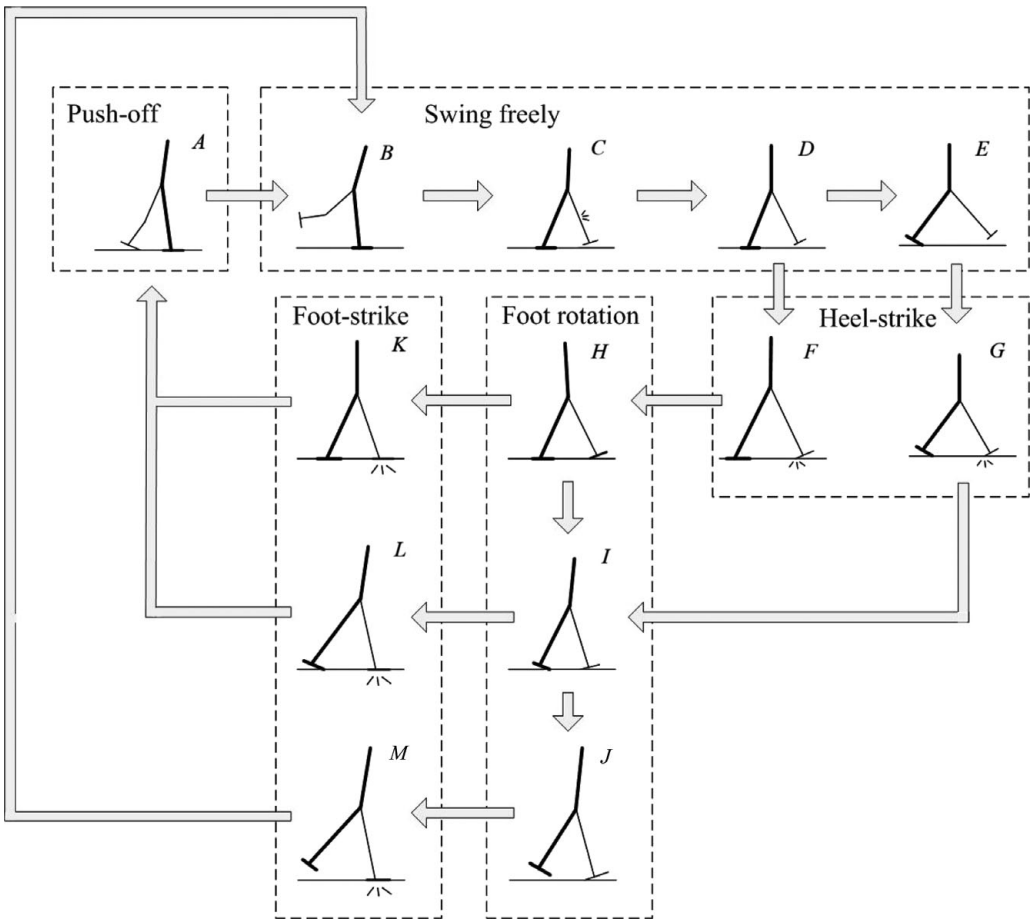

Fig. 3. Walking sequence of the passivity-based biped with flat feet and ankle compliance. The walking sequence has several substreams, which indicate different gaits with corresponding walking phases.

Then, the EoM in matrix format can be obtained from Eqs. (6) and (10):

$$\begin{bmatrix} M_q & -\Phi^{\mathrm{T}} \\ \Phi & 0 \end{bmatrix} \begin{bmatrix} \ddot{q} \\ F_f \end{bmatrix} = \begin{bmatrix} F_q \\ -\dfrac{\partial(\Phi\dot{q})}{\partial q}\dot{q} \end{bmatrix}. \tag{11}$$

The equation of strike moment can be obtained by integration of Eq. (6):

$$M_q\dot{q}^+ = M_q\dot{q}^- + \Phi^{\mathrm{T}} I_f, \tag{12}$$

where $\dot{q}^+$ and $\dot{q}^-$ are the velocities in the generalized coordinates after and before the strike, respectively. Here, I_f is the impulse acted on the walker, which is defined as follows:

$$I_f = \lim_{t^- \to t^+} \int_{t^-}^{t^+} F_f \, \mathrm{d}t. \tag{13}$$

Since the strike is modeled as a fully inelastic impact, the walker satisfies the constraint function $\xi(q)$. Thus, the motion is constrained by the followed equation after the strike:

$$\frac{\partial \xi}{\partial q}\dot{q}^+ = 0. \tag{14}$$

Then, the equation of strike in matrix format can be derived from Eqs. (12) and (14):

$$\begin{bmatrix} M_q & -\Phi^{\mathrm{T}} \\ \Phi & 0 \end{bmatrix} \begin{bmatrix} \dot{q}^+ \\ I_f \end{bmatrix} = \begin{bmatrix} M_q\dot{q}^- \\ 0 \end{bmatrix}. \tag{15}$$

3. Bipedal Walking Gaits

On the basis of the dynamic walking model mentioned above, in this section, we analyzed the possible bipedal walking gaits. Here, different from the existing studies, the series of walking phases is uncertain. The dynamic switching of the walking phase is more close to that of real human walking.

3.1. Walking sequence

The walking sequence of the flat-foot walker is more complicated than that of the round-foot walker.[15,16] When the flat foot strikes the ground, there are two impulses, "heel-strike" and "foot-strike," representing the initial impact of the heel and the following impact as the whole foot contacts the ground. Each foot has three contact cases: foot contact, heel contact, and toe contact. Thus, there appears several substreams in the walking sequence, which is different from the motion of round-foot and point-foot models (see Fig. 3). Note that the sequence in Fig. 3 has several substream.

https://doi.org/10.1017/S0263574711000397 Published online by Cambridge University Press

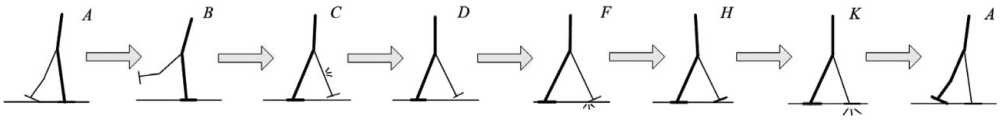

Fig. 4. Walking sequence of gait 1.

One walking step may not include all these phases. Moving to which phase at the bifurcation point is based on the contact force. The direction of the GRF perpendicular to the ground acted on the endpoint of the foot is checked at every simulation step during the motion. The corresponding contact condition is released if the force becomes downward. An impact happens when a new contact is detected. Then, the directions of all the impulsive forces are checked. If an impulsive force is downward, the corresponding constraint is released and the impact is recalculated with the new constraint function.

3.2. Walking phases

As shown in Fig. 3, phase A is the push-off phase, the initial phase of certain gaits. In this phase, the trailing foot rotates around toe with a push-off effect. The foot will lift up when the ground force acting on the toe decreases to zero, which means that the toe loses contact with ground. Then, the walker will move to phase B.

In phase B, C, D, and E, the swing leg of the walker swings freely with no contact with ground. The shank of swing leg is released in phase B. When the shank of the swing leg swings to a relatively small angle, the knee joint is supposed to be locked. There is an impact between shank and thigh of the swing leg in phase C. Then, the shank and the thigh are supposed to be locked in a straight line and the model moves to phase D. If the heel of the trailing foot loses contact with ground before the leading foot strikes ground, the walker will move to phase E, otherwise the walker will move to phase F.

Phases F and G are heel-strike phases. There is an impact between the swing leg and the ground when the heel of the swing leg contacts the ground. The difference between the two phases is the constraint condition of the trailing foot. After the strike, the walker moves to phase H or I.

After heel-strike, the foot of the leading leg rotates around heel. In phase H, the whole trailing foot maintains contact with ground. If the contact force acting on the heel of rear leg decreases to zero, the model will move to phase I. The toe of the rear leg and the heel of the fore leg maintain contact with ground in phase I. If the contact force acting on the toe of the trailing leg decreases to zero, the model will move to phase J in which the whole walker has contact with ground only at the heel of the leading leg.

After foot rotation phases, the walker moves to foot-strike phases, including phase K, L, and M. There is an impact between the whole foot of leading leg and the ground. The difference among the three phases is the constraint of the trailing leg. After foot-strike, the stance leg and the swing leg will be swapped and another walking cycle will begin.

3.3. Walking gaits

According to the walking sequence discussed above, dynamic bipedal walking with flat feet and compliant joints has five possible gaits as follow:

- Gait 1: "$A \to B \to C \to D \to F \to H \to K \to A$" (see Fig. 4). The whole foot of the stance leg keeps contact with ground till the foot-strike of the swing leg occurs. This gait often has a very short step length.
- Gait 2: "$A \to B \to C \to D \to F \to H \to I \to L \to A$" (see Fig. 5). The heel of the stance leg loses contact with ground before the foot-strike of the swing leg occurs. The step length of this gait is relatively small.
- Gait 3: "$B \to C \to D \to F \to H \to I \to J \to M \to B$" (see Fig. 6). The whole foot of the stance leg leaves ground before the foot-strike of the swing leg happens. This gait is quite rare since it has no push-off phase.
- Gait 4: "$A \to B \to C \to D \to E \to G \to I \to L \to A$" (see Fig. 7). The heel of the stance leg loses contact with the ground before the heel-strike of the swing leg, which is called premature heel rise.[20] This gait often has a relatively large step length.
- Gait 5: "$B \to C \to D \to E \to G \to I \to J \to M \to B$" (see Fig. 8). The heel of stance leg leaves ground before heel-strike of swing leg, while the whole stance foot loses contact with ground before the foot-strike of the swing leg occurs. This gait often appears in the large step length walking for stepping over small obstacles or pits. Gaits 2 and 4 are more similar to human normal walking. Gaits 3 and 5 are rare since they have no push-off phases.

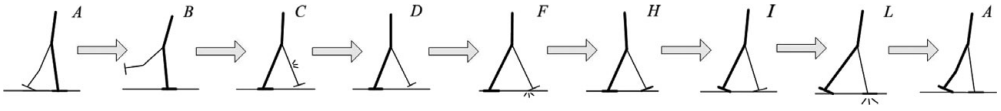

Fig. 5. Walking sequence of gait 2.

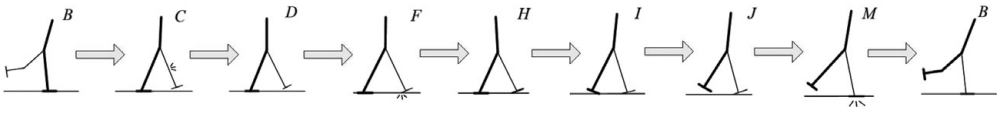

Fig. 6. Walking sequence of gait 3.

https://doi.org/10.1017/S0263574711000397 Published online by Cambridge University Press

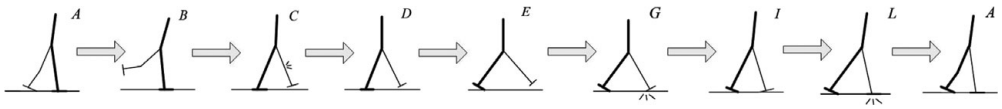

Fig. 7. Walking sequence of gait 4.

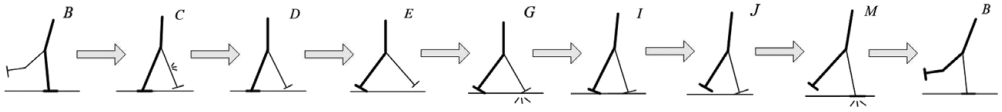

Fig. 8. Walking sequence of gait 5.

3.4. Actuation mode

We add a piecewise constant hip torque to actuate the walker to travel forward on level ground. The hip torque may be different in different phases. The torque is relatively larger in push-off phase (phase A) and double-support phases (phases H, I, and J) to actuate the swing foot to leave ground and compensate the energy loss at heel-strike, and is near zero in the freely swing phase based on the fact that the muscles of the swing leg are generally silent.[13]

Since natural dynamics is an important feature of passivity-based walking, the swing motion of the shank is mainly affected by inertia. Thus, the torsional springs at the knee joints have very low stiffness values, which means that there is little torque at the knee joint.

Torsional springs are added at ankle joints to represent ankle stiffness. Several studies indicate that ankle walking behavior in humans is quite similar to that of a torsional spring.[22–25] To improve the performance of walking and achieve various walking gaits, we set different values of ankle stiffness during the stance phase, which shows a great resemblance with human normal walking[21,27] (see Fig. 9). Similar approach has been used in recent studies.[20] The ankle stiffness has a larger value when the leg has passed the vertical line during the foot-flat phase. During the rest of the stance, the ankle stiffness is lower. The ankle torque changes continuously at the switching of ankle stiffness. In toe-down, foot-flat, and swing phases, the ankle joint reaches equilibrium position when the leg is vertical to foot ($O \rightarrow A$, $A \rightarrow O$, and $B \rightarrow C$ in Fig. 9b). The equilibrium position has a deviation in heel-off phase ($O \rightarrow B$ in Fig. 9b). The foot is supposed to be constrained vertically to the shank to avoid oscillation during swing phase. The ankle does a amount of network as shown by the hatched area in Fig. 9(b), which is taken consider into the calculation of energetic efficiency.

In the simulation, stable cyclic walking is searched for various combination of actuation pattern and ankle stiffness. A typical representative of each gait is chosen for comparison. The hip torques of the representatives of the five gaits are shown in Fig. 10. Both the hip actuation mode and the ankle behavior are predefined with no active control during the walking motion.

4. Experimental Results

All simulations and data processing were performed using Matlab 7 (The Mathworks, Inc., Natick, MA). On the basis of the EoMs mentioned in Section 2, we analyzed the walking

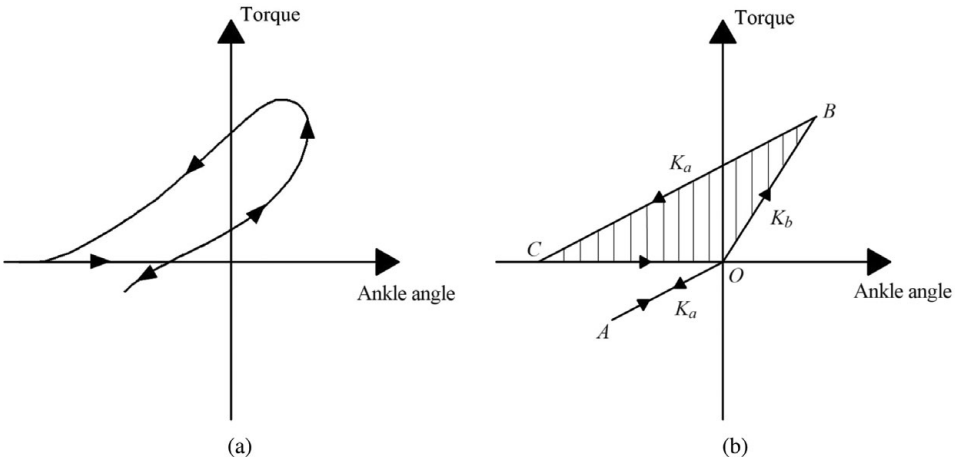

Fig. 9. Comparison of ankle behavior of human normal walking and the proposed model. (a) The torque–angle relationship in ankle joint of human normal walking, adapted from Frigo *et al*.[24] Ankle angle is the relative angle between the shank and the foot. y-axis is the ankle joint torque. (b) The torque–angle relationship in ankle joint of the proposed model. O (the origin point): heel-strike; $O \rightarrow A$: toe-down phase; $A \rightarrow O$: foot-flat phase (the leg is before mid-stance. The ankle stiffness is K_a); $O \rightarrow B$: foot-flat phase (the leg has passed mid-stance and ankle stiffness has a larger value K_b.); $B \rightarrow C$: heel-up phase. The ankle stiffness return to K_a. The line BC is parallel to the line AO; $C \rightarrow O$: swing phase, the foot is reset to the equilibrium position.

https://doi.org/10.1017/S0263574711000397 Published online by Cambridge University Press

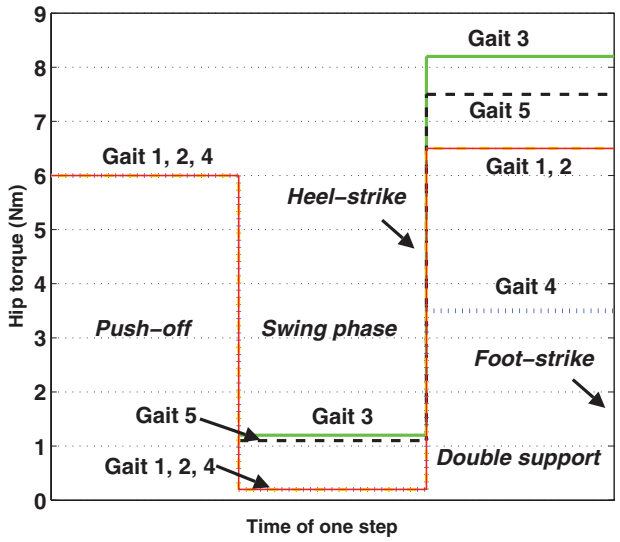

Fig. 10. (Colour online) Actuation pattern for the five gaits. Gaits 1 and 2 have the same patterns, as the two gaits have a lot of similar characteristics. The hip torque of gait 4 is different from gaits 1 and 2 only in the double-support phase. Since gait 3 and gait 5 include no push-off phase, the corresponding parts are absent in the figure.

motion of the biped. The numerical integration of the second-order differential EoMs used the Runge–Kutta method. The actuation mode and ankle behavior are predefined and not changed during the motion.

In this paper, walking efficiency is measured by the nondimensional form of "specific resistance" (energy consumption per kilogram mass per distance traveled per gravity), which is commonly used in the studies of dynamic walking. Note that the energy consumption includes the work done both by the hip torque and the ankle since the change of ankle stiffness injects energy to the walker. The total energy consumption during bipedal walking can be calculated by the following equation:

$$E_{\text{total}} = \sum_{\text{all joints}} \int_0^{T_{\text{total}}} |P\dot{\theta}|\,\mathrm{d}t + E_{\text{ankle}}, \qquad (16)$$

where T_{total} is the total time of walking. P is the joint torque and $\dot{\theta}$ is the joint velocity. E_{ankle} is the work done by the ankle joints, corresponding to the hatched area in Fig. 9(b), which can be calculated by the ankle stiffness.

Parameter values used in the analysis are specified in Table I. All masses and lengths are normalized by the total mass and leg length, respectively.

4.1. Effects of ankle stiffness on gait selection

Our experimental results indicated that ankle stiffness plays an important role in gait selection. Different ankle stiffness may result in different gaits with the same mechanical parameters. The manner of combination of the two ankle stiffness values K_a and K_b has a great influence on the walking gait.

A moderate ratio of K_b to K_a leads to gaits 1 and 2, the walking gaits with short step lengths. We changed the values of K_a and K_b with constant ratio to reveal the effect of magnitude of ankle stiffness on gait selection, which will be illustrated in detail in the following. The results showed that walking with lower ankle stiffness converges to motion of gait 1. The walking characteristics changes gradually as K_a and K_b grow. The stable walking gait changes to gait 2 from gait 1 when ankle stiffness reaches certain critical value.

The model will reach walking with gait 3 when K_a and K_b are close to each other and both have large values. Walking cycles with gaits 4 and 5 can be found in the case of large ratio of K_b to K_a, which means K_b is large while K_a is small.

4.2. Walking characteristics of different gaits

4.2.1. Short step length walking. Gaits 1 and 2 are common gaits with relatively short step lengths, which show great resemblance with human walking. We focused on the comparison of the two gaits. The main difference between gaits 1 and 2 is the motion in foot rotation phases. Experimental results showed that the magnitude of ankle stiffness plays an important role in the selection of the two gaits.

In the experiments, we compared the walking motion under the same mechanical parameters (shown in Table I) but different ankle stiffness. We changed the spring constant for ankle joint spring K_a and K_b with constant ratio ($K_b = 1.8K_a$) to study the effect of ankle stiffness. According to the simulations, the model with small ankle stiffness leads to the stable walking of gait 1, while large ankle stiffness results in the motion cycle of gait 2.

The phase I does not appear if the model has a small value of ankle stiffness. The trailing foot maintains contact with ground when the leading foot rotates with heel. The rear foot begins to lift up after the whole fore foot contacts ground. Consequently, the angle of trailing foot keeps zero before foot-strike, while the angle of leading foot decreases from the value at heel-strike to zero. In this case, the ankle stiffness plays as damping. The model with relatively higher ankle stiffness ($k = 50$ Nm/rad) has a longer time duration in this event (see Fig. 11). The walker will move to phase I from phase H at some moment if ankle stiffness exceeds the

Table I. Parameter values in simulations.

Parameter	Value (−)	Parameter	Value (−)
Leg mass m_l	0.1538	Thigh mass m_t	0.1077
Shank mass m_s	0.0461	Foot mass m_f	0.0355
Upper body mass m_b	0.355	Hip mass m_h	0.2663
Leg length l	1	Thigh length l_t	0.55
Distance from hip joint to CoM of thigh c_t	0.2750	Foot length l_f	0.25
Distance from knee joint to CoM of shank c_s	0.2250	Shank length l_s	0.45
Distance from ankle joint to CoM of foot c_f	0.0250	Upper body length l_b	0.75
Distance from hip joint to CoM of upper body c_b	0.3750	Gravitational acceleration g	9.8 m/s^2

https://doi.org/10.1017/S0263574711000397 Published online by Cambridge University Press

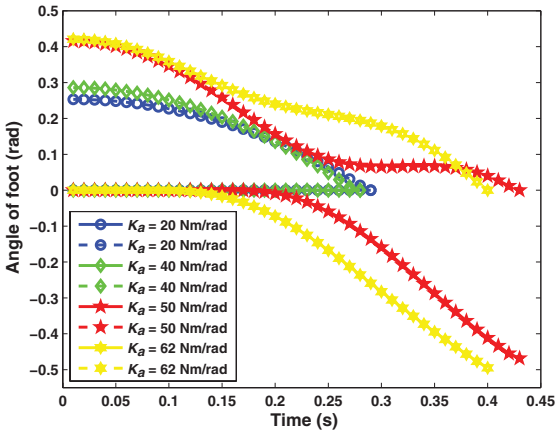

Fig. 11. (Colour online) Angles of feet in foot rotation phase, which are defined as the angles between horizontal axis and each foot with counterclockwise as the positive directions. Time is recorded at heel-strike. Dash lines are leading foot angles while solid lines are trailing foot angles. Relative small ankle stiffness ($K_a = 20$ Nm/rad and $K_a = 40$ Nm/rad) lead to gait 1. Larger ankle stiffness ($K_a = 50$ Nm/rad and $K_a = 62$ Nm/rad) lead to gait 2. The ratio of K_b to K_a is 1.8.

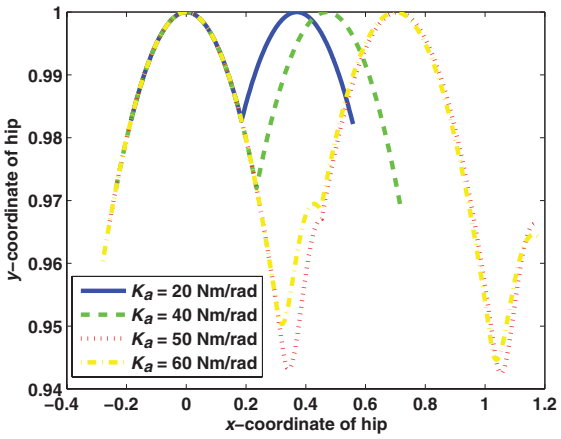

Fig. 12. (Colour online) Hip trajectories of different ankle stiffness. Both x- and y-coordinates are normalized by leg length.

critical value. The rear foot lifts up and rotates around the toe with a negative angle. The walker with larger ankle stiffness moves to phase F earlier.

Hip tracks in two steps of different ankle stiffness are shown in Fig. 12. If walking with gait 1, larger ankle stiffness results in larger step length. Hip tracks of gait 2 have a characteristic of oscillation.

The forces acting on the heel of trailing foot reveal the effect of ankle stiffness on phase transform (Fig. 13). The larger ankle stiffness results in smaller force. The trailing foot will lift up, which means that the model moves to phase I, when the force decreases to zero. If the force does not reach to zero until phase H ends, the walker will not move to phase I.

The energetic efficiency of the models with different ankle stiffness is shown in Fig. 14. Simulation results show that walking in gait 2 is more efficient in average. Efficiency of walking in gait 1 rises as ankle stiffness increases. Ankle stiffness has small influence on energetic efficiency

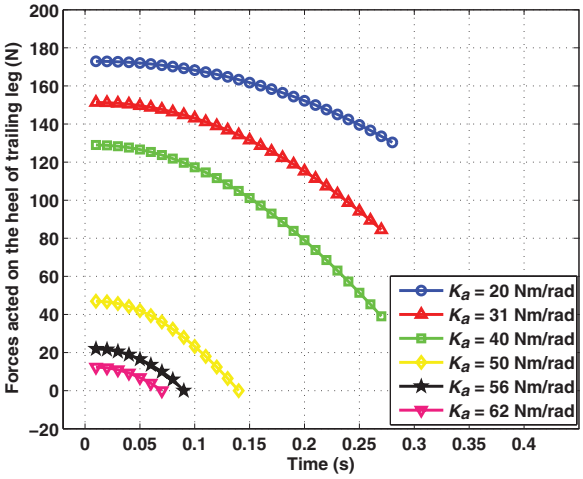

Fig. 13. (Colour online) Force acting on the heel of trailing foot. Time is recorded at heel-strike.

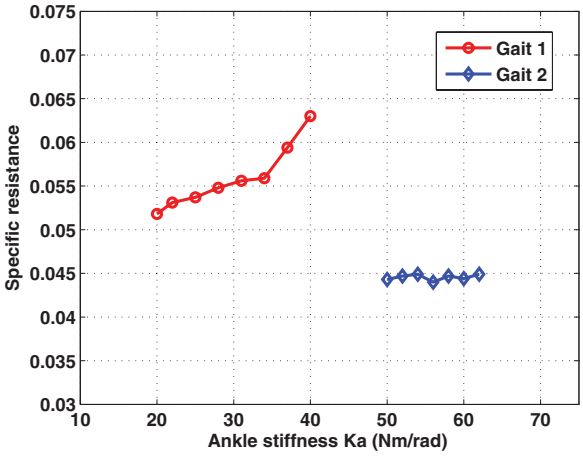

Fig. 14. (Colour online) Energetic efficiency of models with different ankle stiffness. The energy consumption of the bipedal dynamic walking is represented in the nondimensional form of "specific resistance": energy consumption per kilogram mass per distance traveled per gravity.

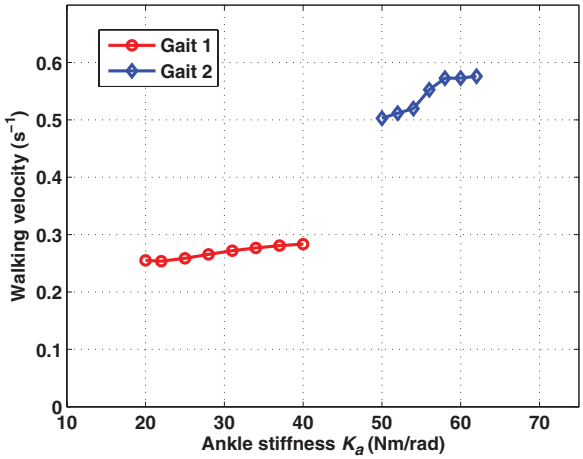

Fig. 15. (Colour online) Velocities of models with different ankle stiffness. The velocities are normalized by leg length.

of walking in gait 2 since the specific resistance changes little.

Figure 15 shows the velocities of models with different ankle stiffness. It indicates that thewalkers with larger ankle

https://doi.org/10.1017/S0263574711000397 Published online by Cambridge University Press

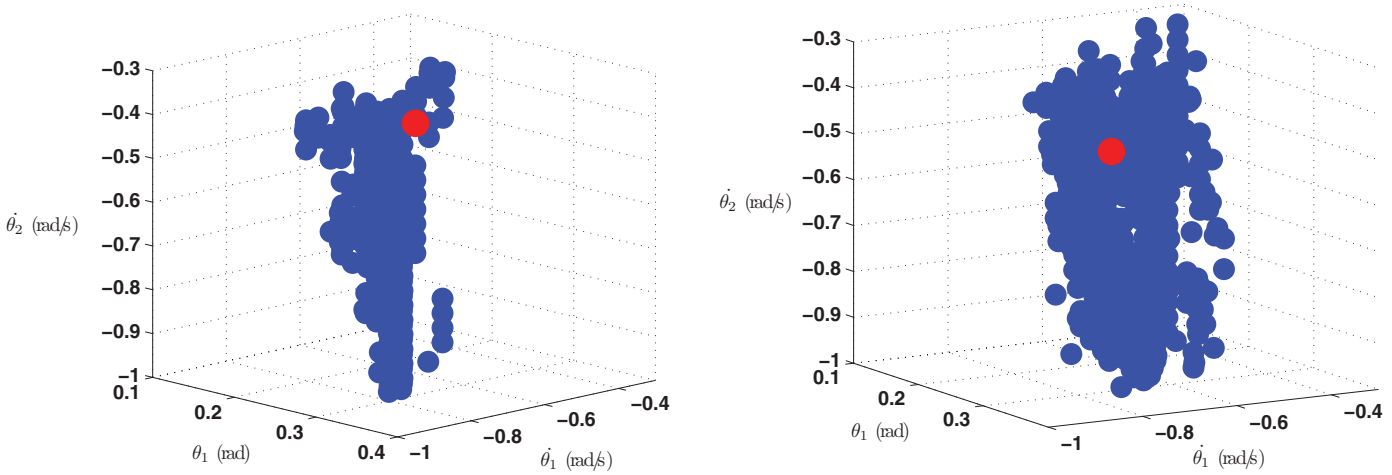

Fig. 16. (Colour online) Basin of attraction of dynamic walking model of different gaits. (a) Basin of attraction of the dynamic walking model with small ankle stiffness ($K_a = 20$ Nm/rad, $K_b = 36$ Nm/rad, gait 1). The blue points represent region of initial conditions that eventually result in the cyclic walking motion. The cyclic motion is indicated with a red point. Parameter values used in the analysis are obtained from Table I. (b) Basin of attraction of the dynamic walking model with large ankle stiffness ($K_a = 50$ Nm/rad, $K_b = 90$ Nm/rad, gait 2). The model has the same mechanical parameters with the model of (a).

stiffness travel faster in both gaits 1 and 2. Walking velocity of gait 2 is larger than that of gait 1 in average.

The stability of the dynamic walking with the two gaits can be analyzed by the approach of limit cycle analysis.[12] We found that walking in gait 2 performs better in global stability than the walking in gait 1. The allowable errors of gait 2 are much larger. This can be inspected by the evaluation of the basin of attraction as shown in Fig. 16, which is the complete set of initial conditions that eventually result in cyclic walking motion.

The leg trajectories of the dynamic walking of gaits 1 and 2 are shown in Fig. 17.

The simulation results described above indicate that walking of gait 2 performs better than walking of gait 1 in efficiency, velocity, and stability.

4.2.2. Other walking gaits. Gaits 3 and 5 are rarely found in real human walking. Gait 4 is the walking with relatively large step length. Walking characteristics of these gaits will be studied in the following paragraphs.

In gait 3, the whole foot of trailing leg leaves ground before foot-strike of leading leg. The model moves to phase J from the bifurcate phase I. Thus, the foot-strike phase is single support followed by Freely swinging phase, which means

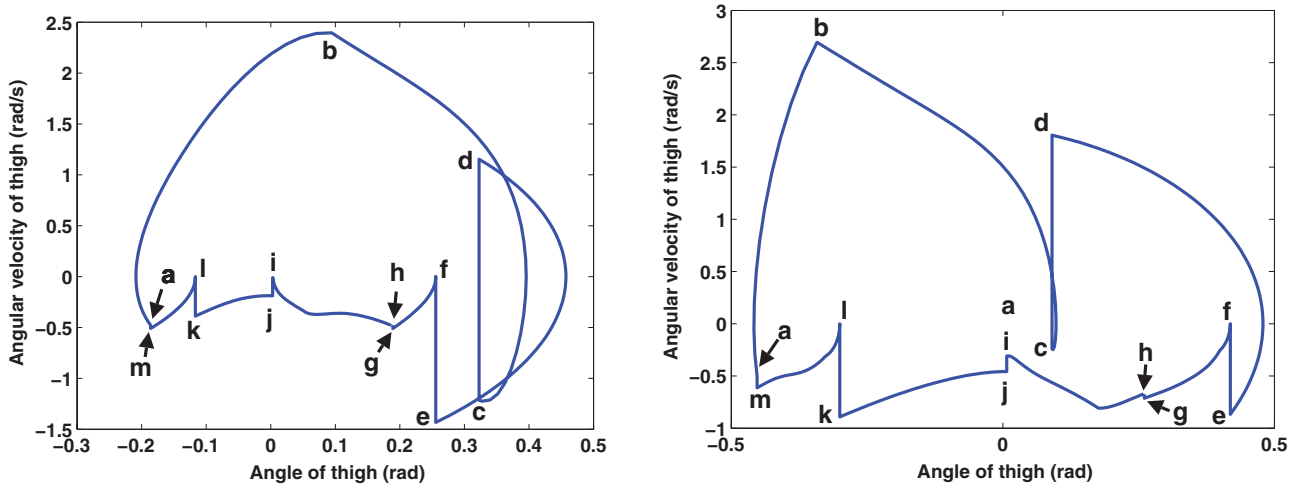

Fig. 17. (Colour online) Leg trajectories of the walkers with different ankle stiffness. (a) The motion cycle of gait 1 with small ankle stiffness ($K_a = 20$ Nm/rad, $K_b = 36$ Nm/rad), while (b) the motion cycle of gait 2 with large ankle stiffness ($K_a = 50$ Nm/rad, $K_b = 90$ Nm/rad). a→b: push-off (phase A). b→c: swing freely (phase B). c→d: knee locking (phase C). d→e: swing freely (phase D). e→f: heel-strike (phase E). f→g: foot rotation. g→h: foot-strike. h→i: the other leg swings freely. i→j: knee locking of the other leg. j→k: the other leg swings freely. k→l: heel-strike of the other leg. l→m: foot rotation. m→a: foot-strike of the other leg.

https://doi.org/10.1017/S0263574711000397 Published online by Cambridge University Press

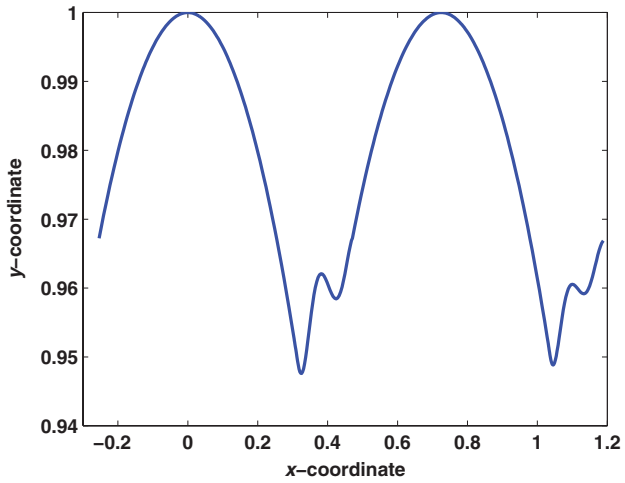

Fig. 18. (Colour online) Hip trajectory of walking in gait 3. Both x- and y-coordinates are normalized by leg length.

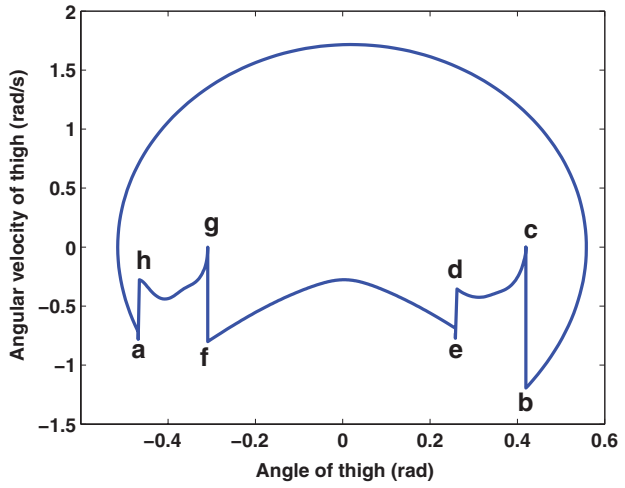

Fig. 19. (Colour online) Leg trajectory of walking in gait 3. a→b: swing freely. b→c: heel-strike. c→d: foot rotation. d→e: knee locking of the other leg. e→f: the other leg swings freely. f→g: heel-strike of the other leg. g→h: foot rotation. h→a: foot-strike of the other leg.

that push-off phase (phase A) is skipped. Generally speaking, the model of gait 3 has lager ankle stiffness than that of gait 2. Leg trajectory and hip track of a typical walking of gait 3 are shown in Figs. 18 and 19, respectively. Ankle stiffness of the model is as follows: $K_a = 93$ Nm/rad, $K_b = 100$ Nm/rad. Mechanical parameters values are obtained from Table I. The normalized walking velocity is $0.3776\,\mathrm{s}^{-1}$. The specific resistance is 0.0498. Both walking velocity and efficiency of gait 3 are between the average values of gaits 1 and 2. The Stability of gait 3 is evaluated by the basin of attraction as shown in Fig. 20. The hip track of gait 3 shows stronger oscillation than that of gaits 1 and 2.

In gait 4, the heel of stance leg loses contact with the ground before heel-strike of the swing leg. The model passes through phases E and G. Leg trajectory and hip track of a typical walking of gait 4 are shown in Figs. 21 and 22, respectively. Ankle stiffness of the model is as follows: $K_a = 35$ Nm/rad, $K_b = 95$ Nm/rad. Mechanical parameter values are obtained from Table I. The normalized walking velocity

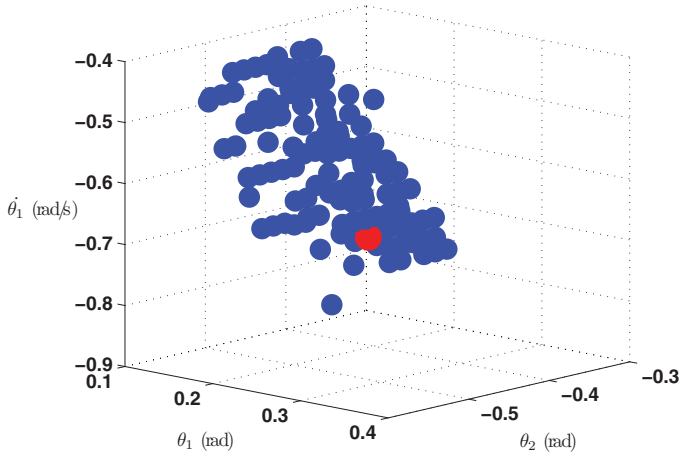

Fig. 20. (Colour online) Basin of attraction of the dynamic walking in gait 3. The blue points represent region of initial conditions that eventually result in the cyclic walking motion. The cyclic motion is indicated with a red point. Parameter values used in the analysis are obtained from Table I.

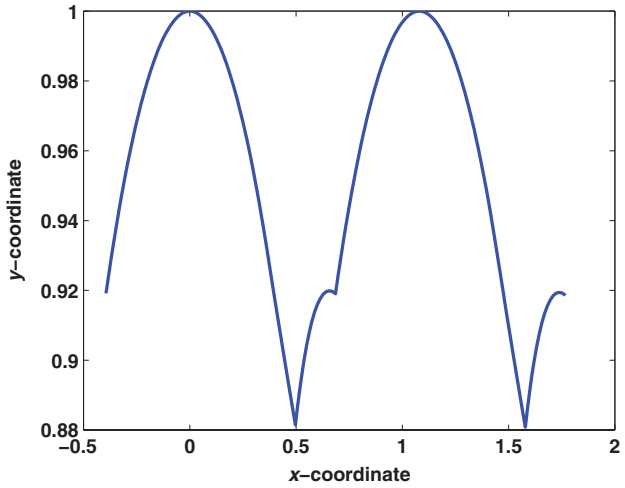

Fig. 21. (Colour online) Hip trajectory of walking in gait 4. Both x- and y-coordinates are normalized by leg length.

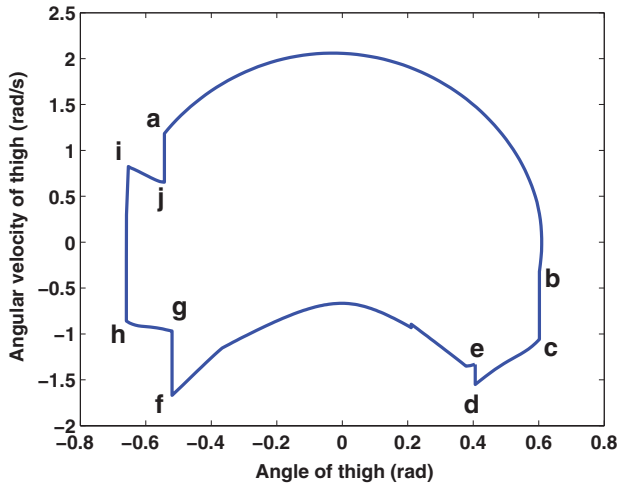

Fig. 22. (Colour online) Leg trajectory of walking in gait 4. a→b: swing freely. b→c: heel-strike. c→d: foot rotation. d→e: foot-strike. e→f: the other leg swings freely. f→g: knee locking of the other leg. g→h: the other leg swings freely. h→i: heel-strike of the other leg. i→j: foot rotation. j→a: foot-strike of the other leg.

https://doi.org/10.1017/S0263574711000397 Published online by Cambridge University Press

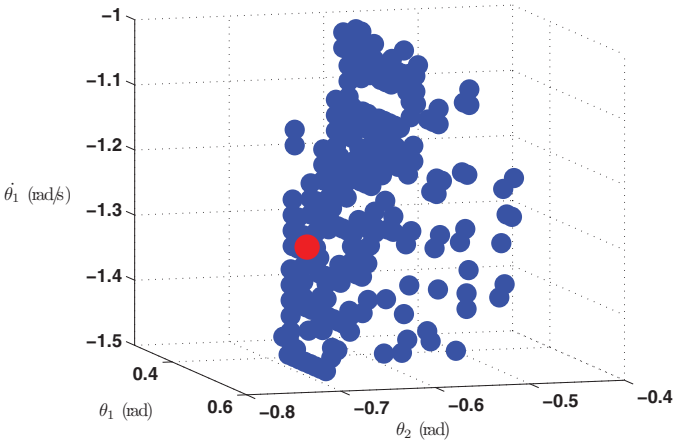

Fig. 23. (Colour online) Basin of attraction of the dynamic walking in gait 4. The blue points represent region of initial conditions that eventually result in the cyclic walking motion. The cyclic motion is indicated with a red point. Parameters values used in the analysis are obtained from Table I.

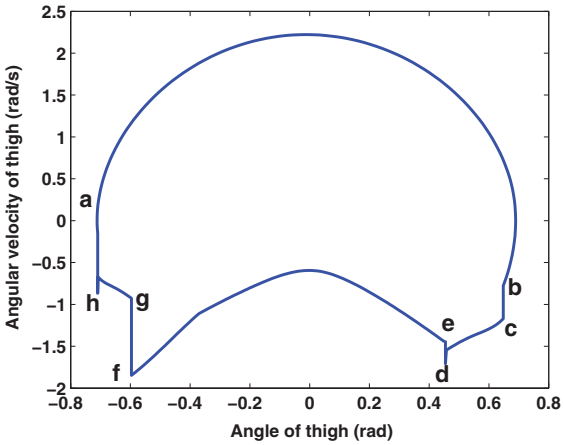

Fig. 25. (Colour online) Leg trajectory of walking in gait 5. a→b: swing freely. b→c: heel-strike. c→d: foot rotation. d→e: foot-strike. e→f: the other leg swings freely. f→g: heel-strike of the other leg. g→h: foot rotation. h→a: foot-strike of the other leg.

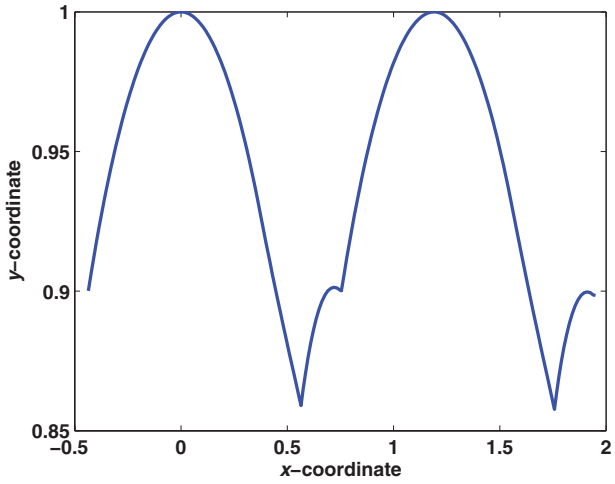

Fig. 24. (Colour online) Hip trajectory of walking in gait 5. Both x- and y-coordinates are normalized by leg length.

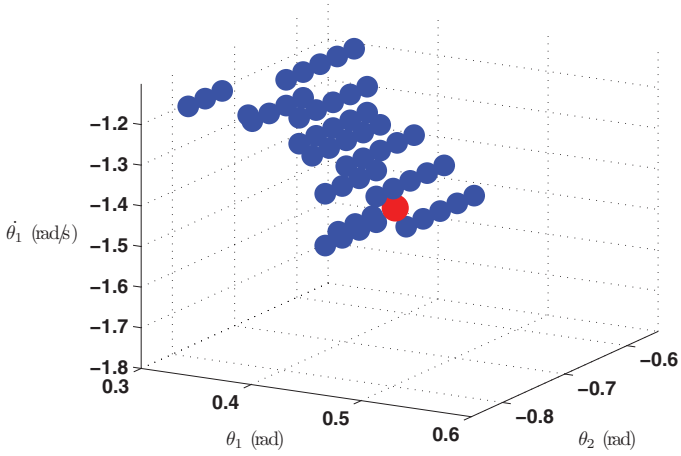

Fig. 26. (Colour online) Basin of attraction of the dynamic walking in gait 5. The blue points represent region of initial conditions that eventually result in the cyclic walking motion. The cyclic motion is indicated with a red point. Parameters values used in the analysis are obtained from Table I.

is $0.9029\,\mathrm{s}^{-1}$. The specific resistance is 0.0432. The walker travels faster in gait 4 than in gaits 1, 2, and 3. Gait 4 also performs well in efficiency and needs lower actuation after heel-strike (See Fig. 10). The main shortcoming of gait 4 is stability, which is also evaluated by the basin of attraction as shown in Fig. 23.

Gait 5 combines the characteristics of foot rotation in gait 3 and heel-strike in gait 4. The heel of stance leg loses contact with the ground before heel-strike of the swing leg. The whole foot of trailing leg leaves ground before foot-strike of leading leg. Gait 5 may be the rarest gait of real human walking. Leg trajectory and hip track of a typical walking of gait 5 are shown in Figs. 24 and 25, respectively. Ankle stiffness of the model is as follows: $K_a = 40\,\mathrm{Nm/rad}$, $K_b = 95\,\mathrm{Nm/rad}$. Mechanical parameters values are obtained from Table I. The normalized walking velocity is $0.8856\,\mathrm{s}^{-1}$, which is comparable with that of gait 4. The specific resistance is 0.1200, which indicates that the efficiency of this gait is much lower than other gaits. The stability is also evaluated by the basin of attraction as shown in Fig. 26.

4.2.3. Comparison. We have evaluated walking characteristics of different gaits above. Then, we compare the performance of all the five gaits. Comparison of step length, walking velocity, and specific resistance are shown in Figs. 27–29, respectively. Models of all the gaits have the same mechanical parameter values obtained from Table I. Ankle stiffness of gaits 3, 4, and 5 are chosen as introduced above. Models with $K_a = 20\,\mathrm{Nm/rad}$, $K_b = 36\,\mathrm{Nm/rad}$ and $K_a = 50\,\mathrm{Nm/rad}$, $K_b = 90\,\mathrm{Nm/rad}$ are selected as the representatives of gaits 1 and 2, respectively.

The results show that step length reflects walking velocity to a certain extent. Gaits 4 and 5 that include phase E and phase G have long step lengths. The speeds of gaits 4 and 5 are much larger than that of other gaits. Contrarily, walking of gait 1 with the shortest step length is the slowest. Comparison of specific resistance shows gait 5 consumes much more energy than other gaits. Gaits 2 and 4 are more efficient. Thus, gait 4 performs well in both velocity and efficiency. However, gaits 3, 4, and 5 have poor stability, which can be found by comparison of the basin of attraction of different gaits. The

https://doi.org/10.1017/S0263574711000397 Published online by Cambridge University Press

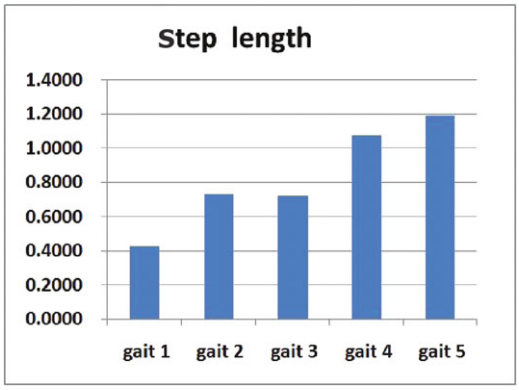

Fig. 27. (Colour online) Step lengths normalized by leg length of different gaits.

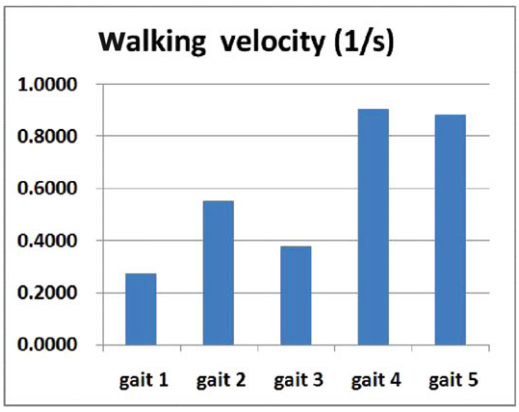

Fig. 28. (Colour online) Walking velocities normalized by leg length of different gaits.

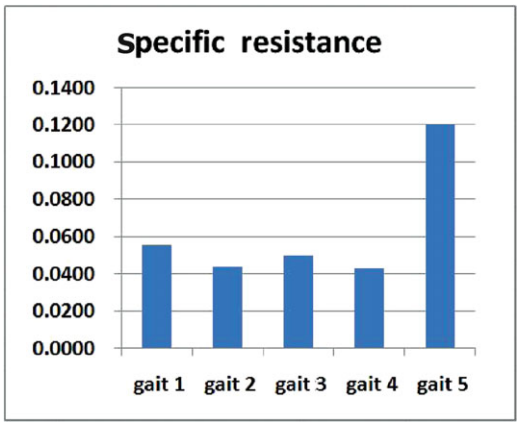

Fig. 29. (Colour online) Specific resistance of different gaits.

allowable errors of gaits 1 and 2 are much larger than that of the other three gaits. Consequently, gaits 2 and 4, which are more close to human walking with the moderate speed, may be the best two gaits in comprehensive characteristics.

5. Discussion

5.1. Effects of ankle stiffness on gait selection

In this study, ankle stiffness plays an important role in gait selection. In dynamic bipedal walking with flat feet and compliant ankle joints, ankle stiffness has great influence on the force states of feet, which determine the constrain condition and phase switching of the model. In long step length gaits (gaits 4 and 5), the ankle stiffness in foot-flat phase, when the stance leg has passed mid-stance (K_b), has a relatively large value. Large K_b produces large ankle torque that pulls heel up, which makes the walker move to phase E from phase D. In addition, gaits 4 and 5 have small K_a, which results in large ankle torque in push-off phase. Thus, the swing leg obtains large angular velocity to travel a long distance over one step. The walking of gait 1 has smaller ankle stiffness, which leads to small ankle joint torque. Therefore, the trailing foot hardly loses contact with ground. The ankle stiffness of gaits 2 and 3 is relatively larger. The corresponding result is that part or whole of the trailing foot loses contact with ground before foot-strike of the leading leg.

The study of the effect of ankle stiffness on gait selection not only shows the influence of force states on phase switching, but also reveals the different roles that ankle stiffness plays in different gaits. In gaits 4 and 5 with large K_b and small K_a, ankle actuation provides large amount of energy to produce fast walking and long step length. In gait 3, large ankle stiffness makes the walker performs as the feet are mounted on legs rigidly. Flexibility plays dominant effect in gait 1. In gait 2, ankle stiffness has a moderate value that obtains a balance of compliance and stiffness.

5.2. Compliant leg and oscillation

Rigid leg model (for example, inverted pendulum model) has been used in various studies of dynamic bipedal walking. Different from walking with rigid leg, compliant leg behavior has been studied recently.[26] For the proposed model in this paper, a leg, which contacts ground at only one point (heel or toe), performs as a compliant leg. The elasticity is not realized by linear spring, but localized at joint level. Thus, the double support phases can be regarded as the model is supported by one rigid leg and one compliant leg (phase A and phase H), two compliant legs (phase I), or only one compliant leg (phase E and phase J). Compared with point-feet and round-feet models, the most important characteristic of flat-feet model is that certain leg performs compliant leg behavior in certain phases. The difference among the gaits is produced by the various combination modes of these phases. Since oscillation is an essential property of elasticity, the track of hip has a characteristic of oscillation in double support phases, especially in large ankle stiffness cases (e.g. gait 3, see Fig. 18). Results show that larger ankle stiffness results in longer time of oscillation.

6. Conclusion

In this paper, we have presented a seven-link dynamic bipedal walking model with compliant joints and flat feet. The model walks forward on level ground with hip and ankle actuation. The bipedal model travels with dynamic series of walking phases due to complicated contact cases of the flat feet. The effects of ankle stiffness on gait selection were studied through simulations. Experimental results showed that ankle stiffness plays different roles in different gaits. Comparison of motion characteristics of different gaits indicated that

https://doi.org/10.1017/S0263574711000397 Published online by Cambridge University Press

long step length usually results in large velocity. The gaits, which are more close to human walking with moderate speed (gaits 2 and 4), achieve better motion characteristics. In certain phases, one or both legs perform compliant behavior. Oscillation can be observed in hip track in double support phases. Modeling and analysis of gait selection of dynamic bipedal walking will make us better understand the walking characteristics of different human gaits and guide more practical bipedal robot prototypes with dynamic walking gaits.

There are several ways to extend this work in the future. Influence of flat foot structure and other parameters also needs to be investigated to obtain more motion characteristics. In addition, the dynamic walking model can be improved by adding certain active control to chose the required gait. Walking with real-time adjustable gaits are more close to real human walking. The control mode and stable transition between different gaits are significant issues to study in future.

Acknowledgments

The authors would like to thank M. Wisse for sharing the simulation files of the Simplest Walking Model. This work was supported by the National Natural Science Foundation of China (No. 61005082, 61020106005), Doctoral Fund of Ministry of Education of China (No. 20100001120005), and the 985 Project of Peking University (No. 3J0865600). This paper was originally submitted under the auspices of the CLAWAR Association. It is an extension of work presented at CLAWAR 2009: The 12th International Conference on Climbing and Walking Robots and the Support Technologies for Mobile Machines, Istanbul, Turkey.

References

1. K. Hirai, M. Hirose, Y. Haikawa and T. Takenaka, "The Development of the Honda Humanoid Robot," *Proceedings of the IEEE International Conference on Robotics and Automation Proceedings*, Leuven, Belgium (1998) pp. 1321–1326.
2. M. Vukobratovic, A. Frank and D. Juricic, "On the stability of biped locomotion," *IEEE Trans. Biomed. Eng.* **17**(1), 25–36 (1970).
3. T. McGeer, "Passive dynamic walking," *Int. J. Robot. Res.* **9**, 68–82 (1990).
4. S. Collins, M. Wisse and A. Ruina, "A three-dimensional passive-dynamic walking robot with two legs and knees," *Int. J. Robot. Res.* **20**, 607–615 (2001).
5. S. Suzuki, K. Furuta and S. Hatakeyama, "Passive walking towards running," *Math. Comput. Modelling Dyn. Syst.* **11**(4), 371–395 (2005).
6. S. Collins, A. Ruina, R. Tedrake and M. Wisse, "Efficient bipedal robots based on passive-dynamic walkers," *Science* **307**, 1082–1085 (2005).
7. M. Wisse, D. G. E. Hobbelen and A. L. Schwab, "Adding an upper body to passive dynamic walking robots by means of a bisecting hip mechanism," *IEEE Trans. Robot.* **23**(1), 112–123 (2007).
8. E. Dertien, "Dynamic walking with dribbel," *IEEE Robot. Autom. Mag.* **13**(3), 118–122 (2006).
9. Y. Harata, F. Asano, Z. Luo, K. Taji and Y. Uno, "Biped gait generation based on parametric excitation by knee-joint actuation," *Robotica* **27**, 1063–1073 (2009).
10. M. Garcia, A. Chatterjee, A. Ruina and M. Coleman, "The simplest walking model: Stability, complexity, and scaling," *ASME J. Biomech. Eng.* **120**, 281–288 (1998).
11. A. D. Kuo, "Energetics of actively powered locomotion using the simplest walking model," *ASME J. Biomech. Eng.* **124**, 113–120 (2002).
12. M. Wisse, A. L. Schwab and F. C. T. Van der Helm, "Passive dynamic walking model with upper body," *Robotica* **22**, 681–688 (2004).
13. S. Mochon and T. A. McMahon, "Ballistic walking," *J. Biomech.* **13**(1), 49–57 (1980).
14. A. Ruina, J. E. A. Bertram and M. Srinivasan, "A collisional model of the energetic cost of support work qualitatively explains leg sequencing in walking and galloping, pseudo-elastic leg behavior in running and the walk-to-run transition," *J. Theor. Biol.* **237**(2), 170–192 (2005).
15. M. Kwan and M. Hubbard, "Optimal foot shape for a passive dynamic biped," *J. Theor. Biol.* **248**, 331–339 (2007).
16. Q. Wang, Y. Huang and L. Wang, "Passive dynamic walking with flat feet and ankle compliance," *Robotica* **28**, 413–425 (2010).
17. Q. Wang, Y. Huang, J. Zhu, L. Wang and D. Lv, "Effects of foot shape on energetic efficiency and dynamic stability of passive dynamic biped with upper body," *Int. J. Human. Robot.* **7**(2), 295–313 (2010).
18. M. Wisse, D. G. E. Hobbelen, R. J. J. Rotteveel, S. O. Anderson and G. J. Zeglin, "Ankle Springs Instead of Arc-Shaped Feet for Passive Dynamic Walkers," *Proceedings of the 2006 IEEE International Conference on Humanoids*, Genova, Italy (2006) pp. 110–116.
19. D. G. E. Hobbelen and M. Wisse, "Ankle Joints and Flat Feet in Dynamic Walking," *Proceedings of the International Conference on Climbing and Walking Robots*, Madrid, Spain (2004) pp. 787–800.
20. D. G. E. Hobbelen and M. Wisse, "Ankle actuation for limit cycle walkers," *Int. J. Robot. Res.* **27**(6), 709–735 (2008).
21. S. K. Au, J. Weber and H. Herr, "Powered ankle-foot prosthesis improves walking metabolic economy," *IEEE Trans. Robot.* **25**(1), 51–66 (2009).
22. P. L. Weiss, R. E. Kearney and I. W. Hunter, "Position dependence of ankle joint dynamicsłi. passive mechanics," *J. Biomech.* **19**(9), 727–735 (1986).
23. P. L. Weiss, R. E. Kearney and I. W. Hunter, "Position dependence of ankle joint dynamicsłii. active mechanics," *J. Biomech.* **19**(9), 737–751 (1986).
24. C. Frigo, P. Crenna and L. M. Jensen, "Moment-angle relationship at lower limb joints during human walking at different velocities," *J. Electromyogr. Kines.* **6**(3), 177–190 (1996).
25. T. Sinkjaer, E. Toft, S. Andreassen and B. C. Hornemann, "Muscle stiffness in human ankle dorsiflexors: Intrinsic and reflex components," *J. Neurophysiol.* **60**(3), 1110–1120 (1988).
26. H. Geyer, A. Seyfarth and R. Blickhan, "Compliant leg behaviour explains basic dynamics of walking and running," *Proc. R. Soc. B* **273**, 2861–2867 (2006).
27. I. W. Hunter and R. E. Kearney, "Dynamics of human ankle stiffness: Variation with mean ankle torque," *J. Biomech.* **15**(10), 747–752 (1982).